



As a consequence, many of the state of the art models tend to be prohibitively large, making them inaccessible to large portions of the research community despite scale still being a driving force in obtaining better performance. To address the high computational cost of inference, a growing body of work has been exploring ways to compress these models. As highlighted by several works [e.g. 9, 10, 11], size is only used as a crutch during the optimisation process, while the final solution requires a fraction of the capacity of the model. A typical approach therefore is to sparsify or prune the neural network after training by eliminating parameters that do not play a vital role in the functional behaviour of the model. Furthermore, there is a growing interest in sparse training [e.g. 12, 13, 14], where the model is regularly pruned or sparsified during training in order to reduce the computational burden.

Compressed or sparse representations are not merely useful to reduce computation. Continual learning, for example, focuses on learning algorithms that operate on non-iid data [e.g. 15, 16, 17]. In this setup, training proceeds sequentially on a set of tasks. The system is expected to accelerate learning on subsequent tasks as well as using newly acquired knowledge to potentially improve on previous problems, all of this while maintaining low memory and computational footprint. This is difficult due to the well studied problem of catastrophic forgetting, where performance on previous tasks deteriorates rapidly when new knowledge is incorporated. Many approaches to this problem require identifying the underlying set of parameters needed to encode the solution to a task in order to freeze or protect them via some form of regularisation. In such a scenario, given constraints on model size, computation and memory, it is advantageous that each learned task occupies as little capacity as possible.

In both scenarios, typically, the share of capacity needed to encode the solution is determined by the learning process itself, with no explicit force to impose frugality. This is in contrast with earlier works on  $L_0$  regularisation that explicitly restrict the learning process to result in sparse and compressible representations [18]. The focus of our work, similar to the  $L_0$  literature, is on how to encourage the learning process to be frugal in terms of parameter usage. However instead of achieving this by adding an explicit penalty, we enhance the “rich get richer” nature of gradient descent. In particular we propose a new parameterisation that ensures steps taken by gradient descent are proportional to the magnitude of the parameters. In other words, parameters with larger magnitudes are allowed to adapt faster in order to represent the required features to solve the task, while smaller magnitude parameters are restricted, making it more likely that they will be irrelevant in representing the learned solution.

## 2 Powerpropagation

The desired proportionality of updates to weight magnitudes can be achieved in a surprisingly simple fashion: In the forward pass of a neural networks, raise the parameters of your model (element-wise) to the  $\alpha$ -th power (where  $\alpha > 1$ ) while preserving the sign. It is easy to see that due to the chain rule of calculus the magnitude of the parameters (raised to  $\alpha - 1$ ) will appear in the gradient computation, scaling the usual update. Therefore, small magnitude parameters receive smaller gradient updates, while larger magnitude parameters receive larger updates, leading to the aforementioned “rich get richer” phenomenon. This simple intuition leads to the name of our method.

More formally, we enforce sparsity through an implicit regulariser that results from reparameterising the model similar to [19, 20]. This line of research builds on previous work on matrix factorisation [e.g. 21, 22]. In [19] a parameterisation of the form  $w = v \odot v - u \odot u$  is used to induce sparsity, where  $\odot$  stands for element-wise multiplication and we need both  $v$  and  $u$  to be able to represent negative values, since the parameters are effectively squared. In our work we rely on a simpler formulation where  $w = v|v|^{\alpha-1}$ , for any arbitrary power  $\alpha \geq 1$  (as compared to fixing  $\alpha$  to 2), which, since we preserved the sign of  $v$ , can represent both negative and positive values. For  $\alpha = 1$  this recovers the standard setting.

If we denote by  $\Theta = \mathcal{R}^M$  the original parameter space or manifold embedded in  $\mathcal{R}^M$ , our reparameterisation can be understood through an invertible map  $\Psi$ , where its inverse  $\Psi^{-1}$  projects  $\theta \in \Theta$  into  $\phi \in \Phi$ , where  $\Phi$  is a new parameter space also embedded in  $\mathcal{R}^M$ , i.e.  $\Phi = \mathcal{R}^M$ . The map is defined by applying the function  $\Psi : \mathcal{R} \rightarrow \mathcal{R}$ ,  $\Psi(x) = x|x|^{\alpha-1}$  element-wise, where by abuse of notation we refer to both the vector and element level function by  $\Psi$ . This new parameter space or manifold  $\Phi$  has a curvature (or metric) that depends on the Jacobian of  $\Psi$ . Similar constructions have

been previously used in optimisation, as for example in the case of the widely known Mirror Descent algorithm [23], where the invertible map  $\Psi$  is the link function. For deep learning, Natural Neural Networks [24] rely on a reparameterisation of the model such that in the new parameter space, at least initially, the curvature is close to the identity matrix, making a gradient descent step similar to a second order step. Warp Gradient Descent [25] relies on a meta-learning framework to learn a nonlinear projection of the parameters with a similar focus of improving efficiency of learning. In contrast, our focus is to construct a parameterisation that leads to an implicit regularisation towards sparse representation, following [19], rather than improving convergence.

Given the form of our mapping  $\Psi$ , in the new parameterisation the original weight  $\theta_i$  will be replaced by  $\phi_i$ , where  $\Psi(\phi_i) = \phi_i |\phi_i|^{\alpha-1} = \theta_i$  and  $i$  indexes over the dimensionality of the parameters. Note that we apply this transformation only to the weights of a neural network, leaving other parameters untouched. Given the reparameterised loss  $\mathcal{L}(\cdot, \Psi(\phi))$ , the gradient wrt. to  $\phi$  becomes

$$\frac{\partial \mathcal{L}(\cdot, \Psi(\phi))}{\partial \phi} = \frac{\partial \mathcal{L}}{\partial \Psi(\phi)} \frac{\partial \Psi(\phi)}{\partial \phi} = \frac{\partial \mathcal{L}}{\partial \Psi(\phi)} \text{diag}(\alpha |\phi|^{\alpha-1}). \quad (1)$$

Note that  $\text{diag}$  indicates a diagonal matrix, and  $|\phi|^{\alpha-1}$  indicates raising element-wise the entries of vector  $|\phi|$  to the power  $\alpha - 1$ .  $\frac{\partial \mathcal{L}}{\partial \Psi(\phi)}$  is the derivative wrt. to the original weight  $\theta = \phi |\phi|^{\alpha-1}$  which is the gradient in the original parameterisation of the model. This is additionally multiplied (element-wise) by the factor  $\alpha |\phi|^{\alpha-1}$ , which will scale the step taken proportionally to the magnitude of each entry. Finally, for clarity, this update is different from simply scaling the gradients in the original parameterisation by the magnitude of the parameter (raised at  $\alpha - 1$ ), since the update is applied to  $\phi$  not  $\theta$ , and is scaled by  $\phi$ . The update rule (1) has the following properties:

- (i) 0 is a critical point for the dynamics of any weight  $\phi_i$ , if  $\alpha > 1$ . This is easy to see as  $\frac{\partial \mathcal{L}}{\partial \phi_i} = 0$  whenever  $\phi_i = 0$  due to the  $\alpha |\phi_i|^{\alpha-1}$  factor.
- (ii) In addition, 0 is surrounded by a plateau and hence weights are less likely to change sign (gradients become vanishingly small in the neighbourhood of 0 due to the scaling). This should negatively affect initialisations that allow for both negative and positive values, but it might have bigger implications for biases.
- (iii) This update is naturally obtained by the Backpropagation algorithm. This comes from the fact that Backpropagation implies applying the chain-rule from the output towards the variable of interest, and our reparameterisation simply adds another composition (step) in the chain before the variable of interest.

At this point the perceptive reader might be concerned about the effect of equation (1) on established practises in the training of deep neural networks. Firstly, an important aspect of reliable training is the initialisation ([e.g. 26, 27, 28]) or even normalisation layers such as batch-norm [29] or layer-norm [30]. We argue that our reparameterisation preserves all properties of typical initialisation schemes as it does not change the function. Specifically, let  $\theta_i \sim p(\theta)$  where  $p(\theta)$  is any distribution of choice. Then our reparameterisation involves initialising  $\phi_i \leftarrow \text{sign}(\theta_i) \cdot \sqrt[\alpha]{|\theta_i|}$ , ensuring the neural network and all intermediary layers are functionally the same. This implies that hidden activations will have similar variance and mean as in the original parameterisation, which is what initialisation and normalisation focus on.

Secondly, one valid question is the impact of modern optimisation algorithms ([e.g. 31, 32, 33]) on our reparameterisation. These approaches correct the gradient step by some approximation of the curvature, typically given by the square root of a running average of squared gradients. This quantity will be proportional (at least approximately) to  $\text{diag}(\alpha |\phi|^{\alpha-1})^1$ . This reflects the fact that our projection relies on making the space more curved and implicitly optimisation harder, which is what these optimisation algorithms aim to fix. Therefore, a naive use with Powerprop. would result in a reduction of the “rich get richer” effect. On the other hand, avoiding such optimisers completely can considerably harm convergence and performance. The reason for this is that they do not only

<sup>1</sup>To see this assume the weights do not change from iteration to iteration. Then each gradient is scaled by the same value  $\text{diag}(\alpha |\phi|^{\alpha-1})$  which factors out in the summation of gradients squared, hence the correction from the optimiser will undo this scaling. In practice  $\phi$  changes over time, though slowly, hence approximately this will still hold.

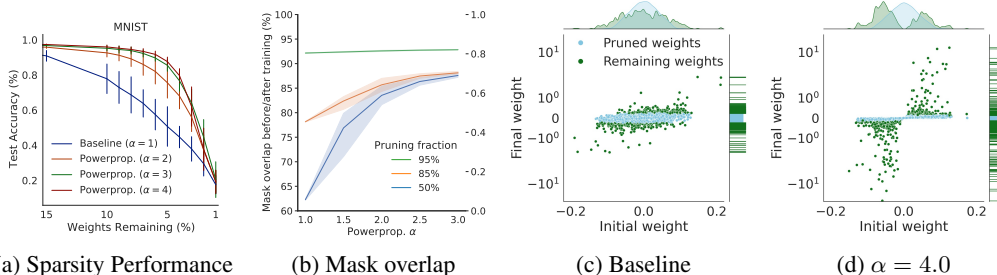


Figure 1: Powerpropagation applied to Image classification. (a) Test accuracy at increasing levels of sparsity for MNIST (b) Overlap between masks computed before and after training (c) & (d) Analysis of weight distributions for a Baseline model and at a high  $\alpha$ . We use 10K weights chosen at random from the network. For a) & b) we show mean and standard deviation over 5 runs. *We provide code to reproduce the MNIST results (a) in the accompanying notebook.*

correct for the curvature induced by our reparameterisation, but also the intrinsic curvature of the problem being solved. Removing the second effect can make optimisation very difficult. We provide empirical evidence of this effect in the Appendix.

To mitigate this issue and make Powerprop. straightforward to use in any setting, we take inspiration from the target propagation literature [34, 35, 36, 37] which proposes an alternative way of thinking about the Backpropagation algorithm.

In our case, we pretend that the exponentiated parameters are the de-facto parameters of the model and compute an update wrt. to them using our optimiser of choice. The updated exponentiated parameters are then seen as a *virtual target*, and we take a gradient descent step on  $\phi$  towards these virtual targets. This will result in a descent step, which, while it relies on modern optimisers to correct for the curvature of the problem, does not correct for the curvature introduced by our parameterisation. Namely if we denote  $optim : \mathcal{R}^M \rightarrow \mathcal{R}^M$  as the function that implements the correction to the gradient done by some modern optimiser, our update becomes  $\Delta\phi = optim \left( \frac{\partial\mathcal{L}}{\partial\Psi(\phi)} \right) \text{diag}(\alpha|\phi|^{\alpha-1})$ .

The proof that our update is indeed correct follows the typical steps taken in the target propagation literature. From a first order Taylor expansion of  $\mathcal{L}(\phi - \eta\Delta\phi)$ , we have that in order for  $\Delta\phi$  to reduce the loss, the following needs to hold:  $\langle \Delta\phi, \frac{\partial\mathcal{L}}{\partial\phi} \rangle > 0$ . But we know that  $\left\langle optim \left( \frac{\partial\mathcal{L}}{\partial\Psi(\phi)} \right), \frac{\partial\mathcal{L}}{\partial\Psi(\phi)} \right\rangle > 0$  as this was a valid step on  $\Psi(\phi)$ . Because  $\text{diag}(\alpha|\phi|^{\alpha-1})$  is positive definite (diagonal matrix with all entries positive), we can multiply it on both sides, proving that  $\langle \Delta\phi, \frac{\partial\mathcal{L}}{\partial\phi} \rangle > 0$ . We provide more details in the Appendix. We will rely on this formulation in our empirical evaluation.

### 3 Effect on weight distribution and sparsification

At this point an empirical demonstration might illuminate the effect of equation (1) on model parameters and our ability to sparsify them. Throughout this work, we will present results from neural networks after the removal of low-magnitude weights. We prune such parameters by magnitude (i.e.  $\min |\theta_i|$ ), following current best practice [e.g. 38, 39, 13]. This is based on a Taylor expansion argument [14] of a sparsely-parameterised function  $f(x, \theta_s)$  which we would like to approximate its dense counterpart  $f(x, \theta)$ :  $f(x, \theta_s) \approx f(\theta, x) + g^T(\theta_s - \theta) + \frac{1}{2}(\theta_s - \theta)^T H(\theta_s - \theta) + \dots$  where  $g$  is the gradient vector and  $H$  the Hessian. As higher order derivatives are impractical to compute for modern networks, minimising the norm of  $(\theta_s - \theta)$  is a practical choice instead.

Following the experimental setup in [10] we study the effect of Powerpropagation at different powers ( $\alpha$ ) relative to standard Backpropagation with otherwise identical settings. Figure 1a shows the effect of increasing sparsity on the layerwise magnitude-pruning setting for LeNet [40] on MNIST [41]. In both cases we notice a significant improvement over an otherwise equivalent baseline. While the choice of  $\alpha$  does influence results, all choices lead to an improvement<sup>2</sup> in the MNIST setting. Where does this improvement come from? Figures 1c & 1d compare weights before and after training

<sup>2</sup>For numerical stability reasons we typically suggest a choice of  $\alpha \in (1, 3]$  depending on the problem.

on MNIST at identical initialisation. We prune the network to 90% and compare the respective weight distributions. Three distinct differences are particularly noticeable: (i) Most importantly, weights initialised close to zero are significantly less likely to survive the pruning process when Powerpropagation is applied (see green Kernel density estimate). (ii) Powerpropagation leads to a heavy-tailed distribution of trained weights, as (1) amplifies the magnitude of such values. These observations are what we refer to as the “rich-get-richer” dynamic of Powerpropagation. (iii) Weights are less likely to change sign (see Figure 1d), as mentioned in Section 2.

One possible concern of (i) and (ii) are that Powerpropagation leads to training procedures where small weights cannot escape pruning, i.e. masks computed at initialisation and convergence are identical. This is undesirable as it is well established that pruning at initialisation is inferior [e.g. 11, 42, 43, 39]. To investigate this we plot the overlap between these masks at different pruning thresholds in Figure 1b. While overlap does increase with  $\alpha$ , at no point do we observe an inability of small weights to escape pruning, alleviating this concern. Code for this motivational example on MNIST is provided.<sup>3</sup>

## 4 Powerpropagation for Continual Learning

### 4.1 Overcoming Catastrophic forgetting

While algorithms for neural network sparsity are well established as a means to reduce training and inference time, we now formalise our argument that such advances can also lead to significant improvements in the continual learning setting: the sequential learning of tasks without forgetting. As this is an inherently resource constraint problem, we argue that many existing algorithms in the literature can be understood as implementing explicit or implicit forms of sparsity. One class of examples are based on weight-space regularisation [e.g. 17, 44] which can be understood as compressing the knowledge of a specific task to a small set of parameters that are forced to remain close to their optimal values. Experience Replay and Coreset approaches [e.g. 45, 46, 47] on the other hand compress data from previous tasks to optimal sparse subsets. The class of methods on which we will base the use of Powerpropagation for Continual Learning on implement gradient sparsity [e.g. 48, 49], i.e. they overcome catastrophic forgetting by explicitly masking gradients to parameters found to constitute the solution to previous tasks.

In particular, let us examine PackNet [48] as a representative of such algorithms. Its underlying principle is simple yet effective: Identify the subnetwork for each task through (iterative) pruning to a fixed budget, then fix the solution for each task by explicitly storing a mask at task switches and protect each such subnetwork by masking gradients from future tasks (using a backward Mask  $\mathcal{M}^b$ ). Given a pre-defined number of tasks  $T$ , PackNet reserves  $1/T$  of the weights. Self-evidently, this procedure benefits from networks that maintain high performance at increased sparsity, which becomes particularly important for large  $T$ . Thus, the application of improved sparsity algorithms such as Powerpropagation are a natural choice. Moreover, PackNet has the attractive property of merely requiring the storage of a binary mask per task, which comes at a cost of 1 bit per parameter, in stark contrast to methods involving the expensive storage (or generative modelling) of data for each past task.

Nevertheless, the approach suffers from its assumption of a known number of maximum tasks  $T$  and its possibly inefficient resource allocation: By reserving a fixed fraction of weights for each task, no distinction is made in terms of difficulty or relatedness to previous data. We overcome both issues through simple yet effective modifications resulting in a method we term *EfficientPacknet* (EPN), shown in Algorithm 1. The key steps common to both methods are (i) Task switch (Line 3), (ii) Training through gradient masking (Line 4), (iii) Pruning (Line 8), (iv) Updates to the backward mask needed to implement gradient sparsity.

Improvements of EPN upon PackNet are: **(a) Lines 7-11:** We propose a simple search over a range of sparsity rates  $S = [s_1, \dots, s_n]$ , terminating the search once the sparse model’s performance falls short of a minimum accepted target performance  $\gamma^P$  (computed on a held-out validation set) or once a minimal acceptable sparsity is reached. While the choice of  $\gamma$  may appear difficult at first, we argue that an maximal acceptable loss in performance is often a natural requirement of a practical engineering application. In addition, in cases where the sparsity rates are difficult to set,

<sup>3</sup><https://github.com/deepmind/deepmind-research/tree/master/powerpropagation>

---

**Algorithm 1:** EfficientPackNet (EPN) + Powerpropagation.

---

**Require:**  $T$  tasks  $[(X_1, y_1), \dots, (X_T, y_T)]$ ; Loss & Eval. functions  $\mathcal{L}, \mathcal{E}$ ; Initial weight distribution  $p(u)$  (e.g. Uniform);  $\alpha$  (for Powerprop.); Target performance  $\gamma \in [0, 1]$ ; Sparsity rates  $S = [s_1, \dots, s_n]$  where  $s_{i+1} > s_i$  and  $s_i \in [0, 1]$ .  
**Output:** Trained model  $\phi$ ; Task-specific Masks  $\{\mathcal{M}^t\}$

```
1  $\mathcal{M}_i^b \leftarrow 1 \forall i$  // Backward mask
2  $\phi_i \leftarrow \text{sign}(\theta) \cdot \sqrt[\alpha]{|\theta_i|}; \theta_i \sim p(\theta)$  // Initialise parameters
3 for  $t \in [1, \dots, T]$  do
4    $\phi \leftarrow \arg \min_{\phi} \mathcal{L}(X_t, y_t, \phi, \mathcal{M}_b)$  // Train on task  $t$  with explicit gradient masking through  $\mathcal{M}_b$ 
5    $P \leftarrow \mathcal{E}(X_t, y_t, \phi)$  // Validation performance of dense model on task  $t$ 
6    $l \leftarrow n$ 
7   do
8      $\mathcal{M}_i^t = \begin{cases} 1 & \text{if } i \in \text{TopK}(\phi, \lfloor s_l \cdot \text{dim}(\phi) \rfloor) \\ 0 & \text{otherwise} \end{cases}$  // Find new Forward mask at sparsity  $s_l$ 
9      $P_s \leftarrow \mathcal{E}(X_T, y_T, \phi \odot \mathcal{M}^t)$  // Validation performance of sparse model
10     $l \leftarrow l - 1$ 
11  while  $P_s > \gamma P \wedge l \geq 1$ ;
12   $\mathcal{M}^b \leftarrow \neg \bigvee_{i=1}^t \mathcal{M}^i$  // Update backward mask to protect all tasks 1, ..., t
13  Re-initialise pruned weights
14  // Optionally retrain with masked weights  $\phi \odot \mathcal{M}^t$  on  $X_t, y_t$  before task switch
14 end
```

---

a computationally efficient binary search (for  $\gamma P$ ) up to a fixed number of steps can be performed instead. Finally, in smaller models the cost of this step may be reduced further by instead using an error estimate based on a Taylor expansion [50]. This helps overcome the inefficient resource allocation of PackNet. **(b) Line 8:** More subtly, we choose the mask for a certain task among all network parameters, including ones used by previous tasks, thus encouraging reuse to existing parameters. PackNet instead forces the use of a fixed number of new parameters, thus possibly requiring more parameters than needed. Thus, the fraction of newly masked weights per task is adaptive to task complexity. **(c) Line 13:** We re-initialise the weights as opposed to leaving them at zero, due to the critical point property (Section 2). While we could leave the weight at their previous value, we found this to lead to slightly worse performance.

Together, these changes make the algorithm more suitable for long sequences of tasks, as we will show in our experiments. In addition, they overcome the assumption of an a priori known number of tasks  $T$ . Another beneficial property of the algorithm is that as the backward pass becomes increasingly sparse, the method becomes more computationally efficient with larger  $T$ .

## 4.2 Task inference during Evaluation

A possible concern for the method presented thus far is the requirement of known task ids at inference time, which are needed to select the correct mask for inputs from an unknown (but previously encountered) problem. This has recently been identified to be a key consideration, distinguishing between the Continual Learning sub-cases of Task-incremental (For classification: With task given, which label?) and Class-incremental learning (Which task and which label?) [51, 52]. Importantly, several methods shown to perform well in the first setting show significant shortcomings when task-ids are not provided.

To overcome this, we propose the use of an unsupervised mask-inference technique recently proposed in [53]: At its core it makes use of a mixture model with each component defined by the subnetwork for task  $t$  (corresponding to mask  $\mathcal{M}^t$ ) and mixture coefficients given by a  $T$ -dimensional vector  $\pi$ :

$$\mathbf{p}(\pi) = f\left(\mathbf{x}, \phi \odot \left(\sum_{t=1}^T \pi_t \mathcal{M}_t\right)\right) \quad (2)$$

where  $\mathbf{x}$  is the input and  $f$  an appropriate function that returns a predictive density (e.g. a softmax). In the absence of an output or task-id associated with  $\mathbf{x}$ , the authors propose the minimisation of the entropy  $\mathcal{H}(\mathbf{p}(\pi))$  as an objective to identify the correct mask. The intuition is that a sub-network operating in the space of the input corresponding to  $\mathbf{x}$ 's task-id should have low entropy. Thus, the negative gradient  $-\frac{\partial \mathcal{H}(\mathbf{p}(\pi))}{\partial \pi}$  with respect to the mixture coefficients provides useful information. In

its more advanced version the procedure then eliminates half of the mixture coefficients (with lowest gradient value) at each step, constructs a new mixture out of the remaining coefficients and repeats the procedure until a single mask remains. The task-id is thus estimated in logarithmic time. This is shown to work well even for thousand of tasks and can be readily combined with Efficient PackNet and Powerpropagation.

It is worth mentioning that the assumption of adequately calibrated predictive confidence in standard neural networks is possibly a naive one given their well-known overconfidence outside the training distribution [e.g. 54]. However, the generality of powerpropagation suggests that it might be readily combined with techniques designed to improve on calibrated uncertainty [e.g. 55, 56] and thus make the suggested inference procedure more robust.

## 5 Related work

Sparsity in Deep Learning has been an active research since at least the first wave of interest in neural networks following Backpropagation [57]. Early work was based on the Hessian [e.g. 58, 50, 59], an attractive but impractical approach in modern architectures. The popularity of magnitude-based pruning dates back to at least [60], whereas iterative pruning was first noted to be effective in [61]. Modern approaches are further categorised as Dense→Sparse or Sparse→Sparse methods, where the first category refers to the instantiation of a dense network that is sparsified throughout the training. Sparse→Sparse algorithms on the other hand maintain constant sparsity throughout, giving them a clear computational advantage.

Among Dense→Sparse methods,  $L_0$  regularisation [18] uses non-negative stochastic gates to penalise non-zero weights during training. Variational Dropout [62] allows for unbounded dropout rates, leading to sparsity. Both are alternatives to magnitude-based pruning. Soft weight threshold reparameterisation [63] is based on learning layerwise pruning thresholds allowing non-uniform budgets across layers. Finally, the authors of [10] observe that re-training weights that previously survived pruning from their initial value can lead to sparsity at superior performance. Examples of Sparse→Sparse methods are Single Shot Network Pruning [64] where an initial mask is chosen according to the salience and kept fixed throughout. In addition, a key insight is to iteratively drop & grow weights while maintaining a fixed sparsity budget. Deep Rewiring for instance [65] augments SGD with a random walk. In addition, weights that are about to change sign are set to zero, activating other weights at random instead. Rigging the Lottery (RigL) [13] instead activates new weights by highest magnitude gradients, whereas Top-KAST [14] maintains two set of masks for (sparse) forward and backward-passes. This also allows the authors to cut the computational budget for gradient computation. In addition, a weight-decay based exploration scheme is used to allow magnitude-based pruning to be used for both masks. Other notable works in this category are Sparse Evolutionary Training [12] and Dynamic sparse reparameterisation [39].

Powerpropagation is also related to Exponentiated Gradient Unnormalized [66] (Example 2) which is a reparameterisation equivalent to setting  $\alpha = 2$ . Indeed, the authors provide a preliminary experiment of the last layer of a convolutional network on MNIST, showing similar inherent sparsity results. We can view Powerprop. as a generalisation of this and related ideas [e.g. 19, 20, 21] with an explicit focus on modern network architectures, introducing necessary practical strategies and demonstrating the competitiveness of reparameterisation approaches at scale.

While continual learning has been studied as early as [15, 16], the work on Elastic Weight Consolidation (EWC) [17] has recently started a resurgence of interest in the field. Contemporary approaches are subdivided into methods relying on regularisation [e.g. 44, 46, 47], data replay [e.g. 67, 68, 45, 69] or architectural approaches [e.g. 70, 71]. Works such as PackNet and SpaceNet [48, 49] have also introduced explicit gradient sparsity as a tool for more efficient continual learning. Other approaches include PathNets which [72] uses evolutionary training to find subnetworks within a larger model for individual tasks.

## 6 Experimental Evaluation

We now provide an experimental comparison of Powerpropagation to a variety of other techniques, both in the sparsity and continual learning settings. Throughout this section we will be guided by three key questions: (i) Can we provide experimental evidence for *inherent sparsity*? (ii) If so, can

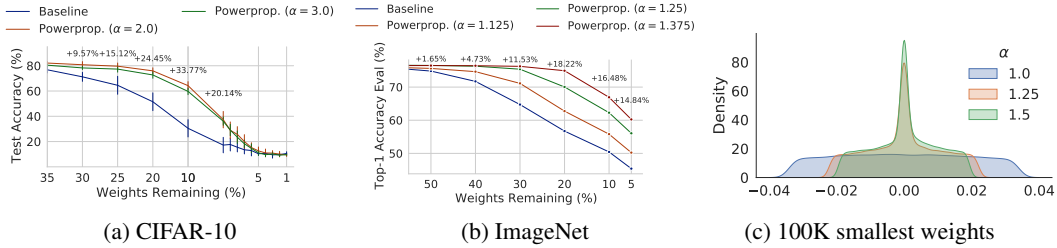


Figure 2: One-shot pruning results on CIFAR-10 (a) and ImageNet (b and c). Performance vs sparsity curves are shown in (a) and (b), highlighting significant improvements wrt. the baseline. This is due to Powerprop.’s effect on the weight distribution, which we show for the smallest 100k weights on ImageNet in (c).  $\alpha > 1$  pushes the weight distribution towards zero, ensuring that more weights can be safely pruned. For CIFAR-10 we show mean and standard deviation over five runs. Repeated runs lead to almost identical results for ImageNet and are thus omitted.

Powerprop. be successfully combined with existing sparsity techniques? (iii) Do improvements brought by Powerprop. translate to measurable advances in Continual Learning? What are strengths and limitations of this strategy?

This section covers varying experimental protocols ranging from supervised image classification to generative modelling and reinforcement learning. Due to space constraints we focus primarily on the interpretation of the results and refer the interested reader to details and best hyperparameters in the Appendix.

## 6.1 Inherent Sparsity

Turning to question (i) first, let us start our investigation by comparing the performance of a pruned method without re-training. This is commonly known as the one-shot pruning setting and is thus a Dense  $\rightarrow$  Sparse method. If Powerprop. does indeed lead to inherently sparse networks its improvement should show most clearly in this setting. Figure 2 shows this comparison for image classification on the popular CIFAR-10 [73] and ImageNet [74] datasets using a smaller version of AlexNet [3] and ResNet50 [4] respectively.<sup>4</sup> In both situations we notice a marked improvement, up to 33% for CIFAR and 18% for ImageNet at specific sparsity rates. In Fig. 2c we show the density of the smallest 100K weights, in which we observe a notable peak around zero for  $\alpha > 1.0$ , providing strong evidence in favour of the inherent sparsity argument. Finally it is worth noting that the choice of  $\alpha$  does influence the optimal learning rate schedule and best results were obtained after changes to the default schedule.

## 6.2 Advanced Pruning

Method	80% Sparsity	90% Sparsity
Iter. Pruning (1.5x)	76.5 [0.84x]	75.2 [0.76x]
RigL (5x)	76.6 $\pm$ 0.06 [1.14x]	75.7 $\pm$ 0.06 [0.52x]
<b>ERK</b>		
RigL (5x)	77.1 $\pm$ 0.06 [2.09x]	76.4 $\pm$ 0.05 [1.23x]
Powerprop. + TopKAST* (2x)	77.51 $\pm$ 0.03 [1.21x]	76.94 $\pm$ 0.10 [0.97x]
Powerprop. + TopKAST* (3x)	<b>77.64</b> $\pm$ 0.05 [1.81x]	<b>77.16</b> $\pm$ 0.19 [1.46x]

Table 2: Extended training. Numbers in square Brackets show FLOPs relative to training of a dense model for a single cycle.

We now address question (ii) by comparing Powerprop. when used in conjunction with and compared to exiting state-of-the-art algorithms on ImageNet. We orient ourselves primarily on the experimental setup in [13] & [14], both of which present techniques among the strongest in the literature. To obtain a Dense $\rightarrow$ Sparse method we combine Powerprop. with Iterative Pruning and combine TopKAST [14] with Powerprop. as our method of choice from the Sparse $\rightarrow$ Sparse literature.

<sup>4</sup>The motivating example in Section 3 also follows this protocol.

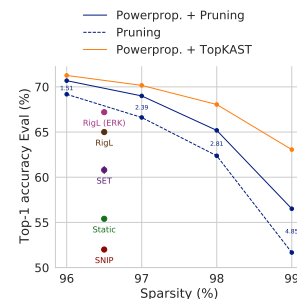


Figure 3: Extreme sparsity

Method	0%				
Dense	76.8 ± 0.09				
	80%	90%	95%	80% (ERK)	90% (ERK)
Static [13]	70.6 ± 0.06	65.8 ± 0.04	59.5 ± 0.11	72.1 ± 0.04	67.7 ± 0.12
DSR [39]	73.3	71.6			
SNFS [38]	74.2	72.3		75.2 ± 0.11	72.9 ± 0.06
SNIP [64]	72.0 ± 0.10	67.2 ± 0.12	57.8 ± 0.40		
RigL [13]	74.6 ± 0.06	72.0 ± 0.05	67.5 ± 0.10	75.1 ± 0.05	73.0 ± 0.04
Iterative pruning [11]	75.6	73.9	70.6		
Iterative pruning (ours)	75.3 ± 0.07	73.7 ± 0.14	70.6 ± 0.05		
Powerprop. + Iter. Pruning	<b>75.7 ± 0.05</b>	<b>74.4 ± 0.02</b>	<b>72.1 ± 0.00</b>		
TopKAST <sup>†</sup> [14]	75.47 ± 0.03	74.65 ± 0.03	<b>72.73 ± 0.10</b>	75.71 ± 0.06	74.79 ± 0.05
Powerprop. + TopKAST <sup>†</sup>	<b>75.75 ± 0.05</b>	<b>74.74 ± 0.04</b>	<b>72.89 ± 0.10</b>	<b>75.84 ± 0.01</b>	<b>74.98 ± 0.09</b>
TopKAST* [14]	76.08 ± 0.02	75.13 ± 0.03	73.19 ± 0.02	76.42 ± 0.03	75.51 ± 0.05
Powerprop. + TopKAST*	<b>76.24 ± 0.07</b>	<b>75.23 ± 0.02</b>	<b>73.25 ± 0.02</b>	<b>76.76 ± 0.08</b>	<b>75.74 ± 0.08</b>

Table 1: Performance of sparse ResNet-50 on Imagenet. Baseline results from [13]. ERK: Erdos-Renyi Kernel [13]. <sup>†</sup>/<sup>\*</sup>: TopKAST at 0%/50% Backward Sparsity. Shown are mean and standard deviation over 3 seeds.

We distinguish between three sub-settings a) Table 1 shows ResNet 50@{80%, 90%, 95%} sparsity, for which the largest number of baseline results are available. We also provide results using the Erdos-Renyi Kernel [13], a redistribution of layerwise sparsity subject to the same fixed overall budget. While this improves results, it increases the floating point operations (FLOPs) at test time. b) Table 2: Extended training, where we scale training steps and learning rate schedule by a factor of the usual 32K steps. While this tends to lead to better results the computational training cost increases. c) Figure 3: Extreme sparsity at 95% – 99% thus testing methods at the limit of what is currently possible. All experiments are repeated 3 times to report mean and standard deviation. As Powerprop. introduces a negligible amount of extra FLOPs (over baseline methods) we only show such values in the extended training setting to provide a fair comparison to the setup in [13]. A longer discussion of a FLOP trade-off can be found in the work on TopKAST [14].

Examining the results, we note that Powerprop. improves both Iterative Pruning & TopKAST in all settings without any modification to the operation of those algorithms. In all settings a large array of other techniques are outperformed. To the best of our knowledge those results constitute a new state-of-the-art performance in all three settings. We emphasise that many of the methods we compare against are based on pruning weights by their magnitude and would thus also be likely to benefit from our method.

### 6.3 Continual Learning

#### 6.3.1 Overcoming Catastrophic forgetting

Algorithm	MNIST	notMNIST
Naive	-258.40	-797.88
Laplace [75, 71]	-108.06	-225.54
EWC [17]	-105.78	-212.62
SI [44]	-111.47	-190.48
VCL [46]	-94.27	-187.34
Eff. PackNet (EPN)	-94.50	-177.08
Powerprop. + Laplace	-96.72	-196.87
Powerprop. + EWC	-95.79	-188.56
Powerprop. + EPN	<b>-92.15</b>	<b>-174.54</b>

Table 3: Results on the Continual generative modelling experiments. Shown is an importance-sampling estimate of the test log-likelihood.

We now turn to question (iii), studying the effectiveness of sparsity methods for Continual Learning. We first consider long task sequences on the Permuted MNIST benchmark, first popularised by [76]. While usually regarded to be an idealised and simple setting, we push its boundaries by drastically

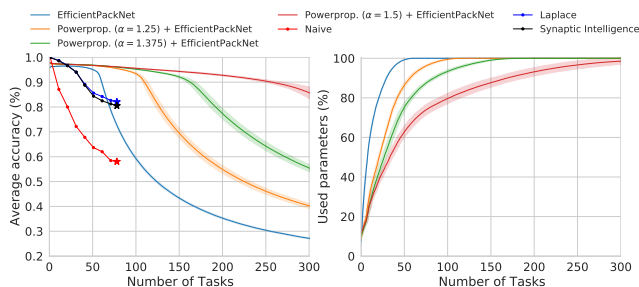


Figure 4: Powerpropagation on extremely long task sequences. **Left:** Average accuracy over all tasks. **Right:** Fraction of unmasked parameters. Shown are mean and standard deviation over 10 repetitions of the experiment.

Table 4: Reinforcement Learning Results on Continual World [79]. Error bars provide 90% confidence intervals.

Method	Avg. success	Forgetting
Fine-tuning	0.00 [0.00, 0.00]	0.87 [0.84, 0.89]
A-GEM [68]	0.02 [0.01, 0.04]	0.89 [0.86, 0.91]
EWC [17]	0.66 [0.61, 0.71]	0.07 [0.04, 0.11]
MAS [83]	0.61 [0.56, 0.66]	-0.01 [-0.04, 0.01]
Perfect Memory	0.36 [0.32, 0.40]	0.07 [0.05, 0.10]
VCL [46]	0.52 [0.47, 0.57]	-0.01 [-0.03, 0.01]
PackNet [48]	0.80 [0.76, 0.84]	0.02 [0.04, 0.00]
Power. + EfficientPackNet ( $\alpha=1.375$ )	0.82 [0.77, 0.87]	0.01 [0.03, 0.01]
Power. + EfficientPackNet ( $\alpha=1.5$ )	<b>0.86</b> [0.82, 0.90]	<b>0.00</b> [-0.02, 0.02]

increasing the number of tasks, which was previously limited to 100 in [77] and 78 in [51], whereas we learn up to 300 in a single model. In all cases we use a network with a single output layer across all tasks, following the protocol by and comparing to [51]. Figure 4 shows the average accuracy and fraction of used weights. We significantly outperform baselines with an average acc. of  $\approx 86\%$  after 300 tasks, whereas the closest baseline (Laplace [71]) falls to 85.61% after merely 51 tasks. This also highlight the effect of  $\alpha$  more noticeably, showing increased performance for higher  $\alpha$ . Note also that the gradient of the used weights curve flattens, showcasing the dynamic allocation of larger number of parameters to tasks early in the sequence, whereas later tasks reuse a larger fraction of previous weights. While we also attempted a comparison with standard PackNet, the model failed, as its default allocation of  $<0.4\%$  of weights per task is insufficient for even a single MNIST task (see Figure 1a). The perspective reader might notice higher performance for considered baselines at small number of tasks. This is due to our choice of  $\gamma = 0.9$  (see Section 4) which we optimise for long sequences. It is worth mentioning that  $\alpha$  can be increased up to a certain limit at which point training for high number of tasks can become unstable. We will investigate this effect in future work.

Moving onto more complex settings, we use Powerprop. on the continual generative modelling experiment in [46] where 10 tasks are created by modelling a single character (using the MNIST and notMNIST<sup>5</sup> datasets) with a variational autoencoder [78]. We report quantitative results in Table 3. In both cases we observe Powerprop. + EfficientPackNet outperforming the baselines. Interestingly, its effectiveness for Catastrophic Forgetting is not limited to PackNet. In particular, we provide results for the Elastic Weight Consolidation (EWC) method and its online version (Laplace) [17, 71] both of which are based on a Laplace approximation (using the diagonal Fisher information matrix). As Powerprop. results in inherently sparse networks, the entries of the diagonal Fisher corresponding to low magnitude weights are vanishingly small (i.e. the posterior distribution has high variance), resulting in virtually no regularisation of those parameters. We observe significant improvements with no other change to the algorithms.

Finally, we move onto Catastrophic Forgetting in Reinforcement Learning using six tasks from the recently published Continual World benchmark [79], a diverse set of realistic robotic manipulation tasks. This is arguably the most complex setting in our Continual Learning evaluation. Following the authors, we use Soft actor-critic [80], training for 1M steps with Adam [33] (relying on the formulation in Section 2) on each task while allowing 100k retrain steps for PackNet (acquiring no additional data during retraining). We report the average success rate (a binary measure based on the distance to the goal) and a forgetting score measuring the difference of current performance to that obtained at the end of training (but importantly before pruning) on a certain task. Thus, if Powerprop. does improve results, this will show in the Forgetting metric. Results are shown in Table 4. Indeed, we notice that a higher  $\alpha$  leads to a reduction of forgetting and hence an overall improvement over PackNet, resulting in superior performance. Finally, it is worth mentioning that (Efficient)PackNet still assume hard task boundaries that are known during training. However, it has previously been shown that it is possible to overcome these limitations using a changepoint detection algorithm [e.g. 81, 82].

<sup>5</sup><http://yaroslavvb.blogspot.com/2011/09/notmnist-dataset.html>

### 6.3.2 Task inference

To provide further insights into question (iii), we now test the task-inference procedure detailed in Section 4.2 in two settings: (1) The class-incremental learning versions of the Permuted- and Split-MNIST benchmark which we take from [51] and (2) The more challenging 10-task Split-CIFAR100 benchmark using an AlexNet-style ConvNet. Note that the protocols between the two benchmark vary slightly, as (2) allows for separate output-layers/heads whereas (1) insists on a single such head. Also, baseline results in (2) do not strictly follow the class-incremental learning setting but are included due to being among the most recent and well-performing results on the benchmark. The choice of these datasets allow us to compare Powerpropagation and EfficientPackNet together with the task-inference procedure against a plethora of published models. In all cases we chose hyperparameters on the validation set first before obtaining test set performance.

Table 5: Class-incremental learning results on Permuted- and Split-MNIST and 10-task Split-CIFAR 100. MNIST baseline results are taken from [51], Split-CIFAR100 results from [84]. Shown are mean and standard deviation over 10 runs for MNIST and 5 runs for CIFAR100.

Algorithm	Permuted-MNIST	Split-MNIST	10-task Split-CIFAR100
<i>Class-incremental learning</i>			
Naive (SGD)	12.82%±0.95	19.46%±0.04%	
EWC [17]	26.32%±4.32	19.80%±0.05%	
Laplace [71]	42.58%±6.50	19.77%±0.04%	
SI [44]	58.52%±4.20	19.67%±0.09%	
MAS [83]	50.81%±2.92	19.52%±0.29%	
LwF [85]	22.64%±0.23	24.17%±1.33%	
EfficientPackNet	97.09%±0.08	99.42%±0.15%	
GEM [86]	96.19%±0.11	96.16%±0.35%	
DGR [67]	95.09%±0.04	95.74%±0.23%	
RtF [87]	97.06%±0.02	97.31%±0.11%	
Powerprop. + EfficientPackNet	<b>97.47% ± 0.05</b>	<b>99.71% ± 0.04%</b>	
<i>Separate heads + Given task-ids</i>			
OWM [88]			50.94% ± 0.60
A-GEM [68]			63.98% ± 1.22
EWC [17]			68.80% ± 0.88
ER_Res [45]			71.73 ± 0.63%
HAT [89]			72.06% ± 0.50
GPM [84]			72.48 ± 0.40%
<i>Separate heads + Task inference</i>			
Powerprop. + EfficientPackNet			<b>73.70 ± 0.70</b>

We note that Powerpropagation + PackNet performs superior in all settings, suggesting that the task-inference procedure works well at least for medium-length task-sequences. To the best of our knowledge, the 10-task Split-Cifar100 results constitute a new state of the art. Hyperparameters for all Continual Learning benchmarks are shown in the Appendix.

## 7 Discussion

In this work we introduced Powerpropagation, demonstrating how its effect on gradients leads to *inherently sparse* networks. As we show in our empirical analyses, Powerprop. is easily combined with existing techniques, often merely requiring a few characters of code to implement. While we show its effect on only a few established algorithms, we hypothesise that a combination with other techniques could lead to further improvements. Bridging gaps between the fields of sparse networks and Continual Learning, we hope that our demonstration of its effect on Catastrophic Forgetting will inspire further interest in such ideas. In terms of future work, we believe that devising automated schemes for learning  $\alpha$  may be worthwhile, making the use of our method even simpler.

Particular attention ought to be paid to its interaction with the learning rate schedule, which we found worthwhile optimising for particular choices of  $\alpha$ . Finally, we also hope further work will bring additional theoretical insights into our method.

## References

- [1] Karl Moritz Hermann, Tomáš Kočiský, Edward Grefenstette, Lasse Espeholt, Will Kay, Mustafa Suleyman, and Phil Blunsom. Teaching machines to read and comprehend. *arXiv preprint arXiv:1506.03340*, 2015.
- [2] Tom B Brown, Benjamin Mann, Nick Ryder, Melanie Subbiah, Jared Kaplan, Prafulla Dhariwal, Arvind Neelakantan, Pranav Shyam, Girish Sastry, Amanda Askell, et al. Language models are few-shot learners. *arXiv preprint arXiv:2005.14165*, 2020.
- [3] Alex Krizhevsky, Ilya Sutskever, and Geoffrey E Hinton. Imagenet classification with deep convolutional neural networks. *Advances in neural information processing systems*, 25:1097–1105, 2012.
- [4] Kaiming He, Xiangyu Zhang, Shaoqing Ren, and Jian Sun. Deep residual learning for image recognition. In *Proceedings of the IEEE conference on computer vision and pattern recognition*, pages 770–778, 2016.
- [5] John Schulman, Sergey Levine, Pieter Abbeel, Michael Jordan, and Philipp Moritz. Trust region policy optimization. In *International conference on machine learning*, pages 1889–1897. PMLR, 2015.
- [6] David Silver, Julian Schrittwieser, Karen Simonyan, Ioannis Antonoglou, Aja Huang, Arthur Guez, Thomas Hubert, Lucas Baker, Matthew Lai, Adrian Bolton, et al. Mastering the game of go without human knowledge. *nature*, 550(7676):354–359, 2017.
- [7] Mikhail Belkin, Daniel Hsu, Siyuan Ma, and Soumik Mandal. Reconciling modern machine-learning practice and the classical bias–variance trade-off. *Proceedings of the National Academy of Sciences*, 116(32):15849–15854, 2019.
- [8] Preetum Nakkiran, Gal Kaplun, Yamini Bansal, Tristan Yang, Boaz Barak, and Ilya Sutskever. Deep double descent: Where bigger models and more data hurt. *arXiv preprint arXiv:1912.02292*, 2019.
- [9] Nal Kalchbrenner, Erich Elsen, Karen Simonyan, Seb Noury, Norman Casagrande, Edward Lockhart, Florian Stimberg, Aaron Oord, Sander Dieleman, and Koray Kavukcuoglu. Efficient neural audio synthesis. In *International Conference on Machine Learning*, pages 2410–2419. PMLR, 2018.
- [10] Jonathan Frankle and Michael Carbin. The lottery ticket hypothesis: Finding sparse, trainable neural networks. *arXiv preprint arXiv:1803.03635*, 2018.
- [11] Trevor Gale, Erich Elsen, and Sara Hooker. The state of sparsity in deep neural networks. *arXiv preprint arXiv:1902.09574*, 2019.
- [12] Decebal Constantin Mocanu, Elena Mocanu, Peter Stone, Phuong H Nguyen, Madeleine Gibescu, and Antonio Liotta. Scalable training of artificial neural networks with adaptive sparse connectivity inspired by network science. *Nature communications*, 9(1):1–12, 2018.
- [13] Utku Evci, Trevor Gale, Jacob Menick, Pablo Samuel Castro, and Erich Elsen. Rigging the lottery: Making all tickets winners. In *International Conference on Machine Learning*, pages 2943–2952. PMLR, 2020.
- [14] Siddhant Jayakumar, Razvan Pascanu, Jack Rae, Simon Osindero, and Erich Elsen. Top-kast: Top-k always sparse training. *Advances in Neural Information Processing Systems*, 33:20744–20754, 2020.
- [15] Anthony Robins. Catastrophic forgetting, rehearsal and pseudorehearsal. *Connection Science*, 7(2):123–146, 1995.
- [16] Robert M French. Catastrophic forgetting in connectionist networks. *Trends in cognitive sciences*, 3(4):128–135, 1999.
- [17] James Kirkpatrick, Razvan Pascanu, Neil Rabinowitz, Joel Veness, Guillaume Desjardins, Andrei A Rusu, Kieran Milan, John Quan, Tiago Ramalho, Agnieszka Grabska-Barwinska, et al.

- Overcoming catastrophic forgetting in neural networks. *Proceedings of the National Academy of Sciences*, page 201611835, 2017.
- [18] Christos Louizos, Max Welling, and Diederik P Kingma. Learning sparse neural networks through  $l_0$  regularization. *arXiv preprint arXiv:1712.01312*, 2017.
- [19] Tomas Vaskevicius, Varun Kanade, and Patrick Rebeschini. Implicit regularization for optimal sparse recovery. In *Advances in Neural Information Processing Systems*, volume 32. Curran Associates, Inc., 2019.
- [20] Peng Zhao, Yun Yang, and Qiao-Chu He. Implicit regularization via hadamard product over-parametrization in high-dimensional linear regression, 2019.
- [21] Suriya Gunasekar, Blake E Woodworth, Srinadh Bhojanapalli, Behnam Neyshabur, and Nati Srebro. Implicit regularization in matrix factorization. In I. Guyon, U. V. Luxburg, S. Bengio, H. Wallach, R. Fergus, S. Vishwanathan, and R. Garnett, editors, *Advances in Neural Information Processing Systems*, volume 30. Curran Associates, Inc., 2017.
- [22] Yuanzhi Li, Tengyu Ma, and Hongyang Zhang. Algorithmic regularization in over-parameterized matrix sensing and neural networks with quadratic activations. In *Proceedings of the 31st Conference On Learning Theory*, pages 2–47, 2018.
- [23] Amir Beck and Marc Teboulle. Mirror descent and nonlinear projected subgradient methods for convex optimization. *Oper. Res. Lett.*, 31(3):167–175, May 2003.
- [24] Guillaume Desjardins, Karen Simonyan, Razvan Pascanu, and koray kavukcuoglu. Natural neural networks. In *Advances in Neural Information Processing Systems*, volume 28, 2015.
- [25] Sebastian Flennerhag, Andrei A. Rusu, Razvan Pascanu, Francesco Visin, Hujun Yin, and Raia Hadsell. Meta-learning with warped gradient descent. In *International Conference on Learning Representations*, 2020.
- [26] Yann A LeCun, Léon Bottou, Genevieve B Orr, and Klaus-Robert Müller. Efficient backprop. In *Neural networks: Tricks of the trade*, pages 9–48. Springer, 2012.
- [27] Xavier Glorot and Yoshua Bengio. Understanding the difficulty of training deep feedforward neural networks. In *Proceedings of the thirteenth international conference on artificial intelligence and statistics*, pages 249–256. JMLR Workshop and Conference Proceedings, 2010.
- [28] Kaiming He, Xiangyu Zhang, Shaoqing Ren, and Jian Sun. Delving deep into rectifiers: Surpassing human-level performance on imagenet classification. In *Proceedings of the IEEE international conference on computer vision*, pages 1026–1034, 2015.
- [29] Sergey Ioffe and Christian Szegedy. Batch normalization: Accelerating deep network training by reducing internal covariate shift. In *International conference on machine learning*, pages 448–456. PMLR, 2015.
- [30] Jimmy Lei Ba, Jamie Ryan Kiros, and Geoffrey E Hinton. Layer normalization. *arXiv preprint arXiv:1607.06450*, 2016.
- [31] John Duchi, Elad Hazan, and Yoram Singer. Adaptive subgradient methods for online learning and stochastic optimization. *Journal of machine learning research*, 12(7), 2011.
- [32] Geoffrey Hinton, Nitish Srivastava, and Kevin Swersky. Neural networks for machine learning lecture 6a overview of mini-batch gradient descent. *Cited on*, 14(8), 2012.
- [33] Diederik P Kingma and Jimmy Ba. Adam: A method for stochastic optimization. *arXiv preprint arXiv:1412.6980*, 2014.
- [34] Yann LeCun. Learning process in an asymmetric threshold network. In *Disordered Systems and Biological Organization*, pages 233–240. Springer Berlin Heidelberg, 1986.
- [35] Yann Lecun. *PhD thesis: Modeles connexionnistes de l'apprentissage (connectionist learning models)*. Universite P. et M. Curie (Paris 6), June 1987.
- [36] Miguel Carreira-Perpinan and Weiran Wang. Distributed optimization of deeply nested systems. In *Proceedings of the Seventeenth International Conference on Artificial Intelligence and Statistics*, pages 10–19, 2014.
- [37] Dong-Hyun Lee, Saizheng Zhang, Antoine Biard, and Yoshua Bengio. Target propagation. In Yoshua Bengio and Yann LeCun, editors, *3rd International Conference on Learning Representations, ICLR 2015, San Diego, CA, USA, May 7-9, 2015, Workshop Track Proceedings*, 2015.

- [38] Tim Dettmers and Luke Zettlemoyer. Sparse networks from scratch: Faster training without losing performance. *arXiv preprint arXiv:1907.04840*, 2019.
- [39] Hesham Mostafa and Xin Wang. Parameter efficient training of deep convolutional neural networks by dynamic sparse reparameterization. In *International Conference on Machine Learning*, pages 4646–4655. PMLR, 2019.
- [40] Yann LeCun, Bernhard Boser, John S Denker, Donnie Henderson, Richard E Howard, Wayne Hubbard, and Lawrence D Jackel. Backpropagation applied to handwritten zip code recognition. *Neural computation*, 1(4):541–551, 1989.
- [41] Yann LeCun, Corinna Cortes, and CJ Burges. Mnist handwritten digit database. *ATT Labs [Online]*. Available: <http://yann.lecun.com/exdb/mnist>, 2, 2010.
- [42] Utku Evci, Fabian Pedregosa, Aidan Gomez, and Erich Elsen. The difficulty of training sparse neural networks. *arXiv preprint arXiv:1906.10732*, 2019.
- [43] Jonathan Frankle, Gintare Karolina Dziugaite, Daniel M Roy, and Michael Carbin. The lottery ticket hypothesis at scale. *arXiv preprint arXiv:1903.01611*, 8, 2019.
- [44] Friedemann Zenke, Ben Poole, and Surya Ganguli. Continual learning through synaptic intelligence. *arXiv preprint arXiv:1703.04200*, 2017.
- [45] David Rolnick, Arun Ahuja, Jonathan Schwarz, Timothy P Lillicrap, and Greg Wayne. Experience replay for continual learning. *arXiv preprint arXiv:1811.11682*, 2018.
- [46] Cuong V Nguyen, Yingzhen Li, Thang D Bui, and Richard E Turner. Variational continual learning. *arXiv preprint arXiv:1710.10628*, 2017.
- [47] Michalis K Titsias, Jonathan Schwarz, Alexander G de G Matthews, Razvan Pascanu, and Yee Whye Teh. Functional regularisation for continual learning with gaussian processes. *arXiv preprint arXiv:1901.11356*, 2019.
- [48] Arun Mallya and Svetlana Lazebnik. Packnet: Adding multiple tasks to a single network by iterative pruning. In *Proceedings of the IEEE Conference on Computer Vision and Pattern Recognition*, pages 7765–7773, 2018.
- [49] Ghada Sokar, Decebal Constantin Mocanu, and Mykola Pechenizkiy. Spacenet: Make free space for continual learning. *Neurocomputing*, 439:1–11, 2021.
- [50] Yann LeCun, John S Denker, and Sara A Solla. Optimal brain damage. In *Advances in neural information processing systems*, pages 598–605, 1990.
- [51] Yen-Chang Hsu, Yen-Cheng Liu, Anita Ramasamy, and Zsolt Kira. Re-evaluating continual learning scenarios: A categorization and case for strong baselines. *arXiv preprint arXiv:1810.12488*, 2018.
- [52] Gido M Van de Ven and Andreas S Tolias. Three scenarios for continual learning. *arXiv preprint arXiv:1904.07734*, 2019.
- [53] Mitchell Wortsman, Vivek Ramanujan, Rosanne Liu, Aniruddha Kembhavi, Mohammad Rastegari, Jason Yosinski, and Ali Farhadi. Supermasks in superposition. *arXiv preprint arXiv:2006.14769*, 2020.
- [54] Ian J Goodfellow, Jonathon Shlens, and Christian Szegedy. Explaining and harnessing adversarial examples. *arXiv preprint arXiv:1412.6572*, 2014.
- [55] Charles Blundell, Julien Cornebise, Koray Kavukcuoglu, and Daan Wierstra. Weight uncertainty in neural network. In *International Conference on Machine Learning*, pages 1613–1622. PMLR, 2015.
- [56] Balaji Lakshminarayanan, Alexander Pritzel, and Charles Blundell. Simple and scalable predictive uncertainty estimation using deep ensembles. *arXiv preprint arXiv:1612.01474*, 2016.
- [57] David E Rumelhart, Geoffrey E Hinton, and Ronald J Williams. Learning internal representations by error propagation. Technical report, California Univ San Diego La Jolla Inst for Cognitive Science, 1985.
- [58] Michael C Mozer and Paul Smolensky. Skeletonization: A technique for trimming the fat from a network via relevance assessment. In *Advances in neural information processing systems*, pages 107–115, 1989.

- [59] Babak Hassibi and David G Stork. *Second order derivatives for network pruning: Optimal brain surgeon*. Morgan Kaufmann, 1993.
- [60] Georg Thimm and Emile Fiesler. Evaluating pruning methods. In *Proceedings of the International Symposium on Artificial neural networks*, pages 20–25. Citeseer, 1995.
- [61] Nikko Ström. Sparse connection and pruning in large dynamic artificial neural networks. In *Fifth European Conference on Speech Communication and Technology*, 1997.
- [62] Dmitry Molchanov, Arsenii Ashukha, and Dmitry Vetrov. Variational dropout sparsifies deep neural networks. In *International Conference on Machine Learning*, pages 2498–2507. PMLR, 2017.
- [63] Aditya Kusupati, Vivek Ramanujan, Raghav Somani, Mitchell Wortsman, Prateek Jain, Sham Kakade, and Ali Farhadi. Soft threshold weight reparameterization for learnable sparsity. In *International Conference on Machine Learning*, pages 5544–5555. PMLR, 2020.
- [64] Namhoon Lee, Thalaiyasingam Ajanthan, and Philip HS Torr. Snip: Single-shot network pruning based on connection sensitivity. *arXiv preprint arXiv:1810.02340*, 2018.
- [65] Guillaume Bellec, David Kappel, Wolfgang Maass, and Robert Legenstein. Deep rewiring: Training very sparse deep networks. *arXiv preprint arXiv:1711.05136*, 2017.
- [66] Ehsan Amid and Manfred K Warmuth. Reparameterizing mirror descent as gradient descent. *Advances in Neural Information Processing Systems*, 2020. Version 1 of the article (<https://arxiv.org/abs/2002.10487v1>) contains experiments with the last layer of a neural network.
- [67] Hanul Shin, Jung Kwon Lee, Jaehong Kim, and Jiwon Kim. Continual learning with deep generative replay. *arXiv preprint arXiv:1705.08690*, 2017.
- [68] Arslan Chaudhry, Marc’ Aurelio Ranzato, Marcus Rohrbach, and Mohamed Elhoseiny. Efficient lifelong learning with a-gem. *arXiv preprint arXiv:1812.00420*, 2018.
- [69] Christos Kaplanis, Claudia Clopath, and Murray Shanahan. Continual reinforcement learning with multi-timescale replay. *arXiv preprint arXiv:2004.07530*, 2020.
- [70] Andrei A Rusu, Neil C Rabinowitz, Guillaume Desjardins, Hubert Soyer, James Kirkpatrick, Koray Kavukcuoglu, Razvan Pascanu, and Raia Hadsell. Progressive neural networks. *arXiv preprint arXiv:1606.04671*, 2016.
- [71] Jonathan Schwarz, Jelena Luketina, Wojciech M Czarnecki, Agnieszka Grabska-Barwinska, Yee Whye Teh, Razvan Pascanu, and Raia Hadsell. Progress & compress: A scalable framework for continual learning. *arXiv preprint arXiv:1805.06370*, 2018.
- [72] Chrisantha Fernando, Dylan Banarse, Charles Blundell, Yori Zwols, David Ha, Andrei A Rusu, Alexander Pritzel, and Daan Wierstra. Pathnet: Evolution channels gradient descent in super neural networks. *arXiv preprint arXiv:1701.08734*, 2017.
- [73] Alex Krizhevsky, Geoffrey Hinton, et al. Learning multiple layers of features from tiny images. 2009.
- [74] Olga Russakovsky, Jia Deng, Hao Su, Jonathan Krause, Sanjeev Satheesh, Sean Ma, Zhiheng Huang, Andrej Karpathy, Aditya Khosla, Michael Bernstein, et al. Imagenet large scale visual recognition challenge. *International journal of computer vision*, 115(3):211–252, 2015.
- [75] Eleazar Eskin, Alex J Smola, and SVN Vishwanathan. Laplace propagation. In *Advances in neural information processing systems*, pages 441–448, 2004.
- [76] Ian J Goodfellow, Mehdi Mirza, Da Xiao, Aaron Courville, and Yoshua Bengio. An empirical investigation of catastrophic forgetting in gradient-based neural networks. *arXiv preprint arXiv:1312.6211*, 2013.
- [77] Hippolyt Ritter, Aleksandar Botev, and David Barber. Online structured laplace approximations for overcoming catastrophic forgetting. *arXiv preprint arXiv:1805.07810*, 2018.
- [78] Diederik P Kingma and Max Welling. Auto-encoding variational bayes. *arXiv preprint arXiv:1312.6114*, 2013.
- [79] Maciej Wolczyk, Michal Zajac, Razvan Pascanu, Lukasz Kucinski, and Piotr Milos. Continual world: A robotic benchmark for continual reinforcement learning. *arXiv preprint arXiv:2105.10919*, 2021.

- [80] Tuomas Haarnoja, Aurick Zhou, Pieter Abbeel, and Sergey Levine. Soft actor-critic: Off-policy maximum entropy deep reinforcement learning with a stochastic actor. In *International Conference on Machine Learning*, pages 1861–1870. PMLR, 2018.
- [81] Kieran Milan, Joel Veness, James Kirkpatrick, Michael Bowling, Anna Koop, and Demis Hassabis. The forget-me-not process. *Advances in Neural Information Processing Systems*, 29:3702–3710, 2016.
- [82] Ryan Prescott Adams and David JC MacKay. Bayesian online changepoint detection. *arXiv preprint arXiv:0710.3742*, 2007.
- [83] Rahaf Aljundi, Francesca Babiloni, Mohamed Elhoseiny, Marcus Rohrbach, and Tinne Tuytelaars. Memory aware synapses: Learning what (not) to forget. In *Proceedings of the European Conference on Computer Vision (ECCV)*, pages 139–154, 2018.
- [84] Gobinda Saha, Isha Garg, and Kaushik Roy. Gradient projection memory for continual learning. *arXiv preprint arXiv:2103.09762*, 2021.
- [85] Zhizhong Li and Derek Hoiem. Learning without forgetting. *IEEE Transactions on Pattern Analysis and Machine Intelligence*, 2017.
- [86] David Lopez-Paz et al. Gradient episodic memory for continual learning. In *Advances in Neural Information Processing Systems*, pages 6470–6479, 2017.
- [87] Gido M Van de Ven and Andreas S Tolias. Generative replay with feedback connections as a general strategy for continual learning. *arXiv preprint arXiv:1809.10635*, 2018.
- [88] Guanxiong Zeng, Yang Chen, Bo Cui, and Shan Yu. Continual learning of context-dependent processing in neural networks. *Nature Machine Intelligence*, 1(8):364–372, 2019.
- [89] Joan Serra, Didac Suris, Marius Miron, and Alexandros Karatzoglou. Overcoming catastrophic forgetting with hard attention to the task. In *International Conference on Machine Learning*, pages 4548–4557. PMLR, 2018.
- [90] Priya Goyal, Piotr Dollár, Ross Girshick, Pieter Noordhuis, Lukasz Wesolowski, Aapo Kyrola, Andrew Tulloch, Yangqing Jia, and Kaiming He. Accurate, large minibatch sgd: Training imagenet in 1 hour. *arXiv preprint arXiv:1706.02677*, 2017.
- [91] Tianhe Yu, Deirdre Quillen, Zhanpeng He, Ryan Julian, Karol Hausman, Chelsea Finn, and Sergey Levine. Meta-world: A benchmark and evaluation for multi-task and meta reinforcement learning. In *Conference on Robot Learning*, pages 1094–1100. PMLR, 2020.

## A Powerpropagation with modern optimisers

Figure 5 shows an empirical evaluation on MNIST relating to our discussion of modern optimisation algorithms in Section 2. We compare Adam [33] (with a learning rate of  $10^{-3}$ ) applied to Powerpropagation a) directly to compute  $\frac{d\mathcal{L}}{dW}$  and our proposed version b)  $Adam(\frac{d\mathcal{L}}{dW^*}) \cdot \frac{dW^*}{dW}$  where we denote by  $W^*$  the re-parameterised version of  $W$ . For completeness, we also include a standard classifier not using Powerpropagation trained with Adam.

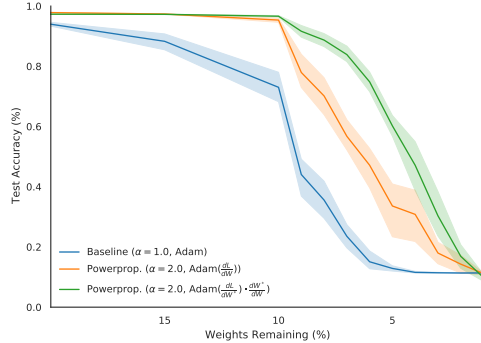


Figure 5: Shown are mean and standard deviation over five random seeds.

We note that performance of our alternative gradient computation indeed performs better than vanilla Adam. Nevertheless, its distinct improvement over the baseline is notable, suggesting that the issue pointed out in Section 2 may be less severe than expected. We hypothesise this is due to the moving average computation of Adam, suggesting Adam is unable to completely undo the “rich get richer” dynamics introduced by Powerpropagation, underestimating the correction at every point. This suggests that Adam’s parameters ( $\beta_1, \beta_2$ ) may play an important role. We leave this investigation for future work and recommend our computation  $Adam(\frac{d\mathcal{L}}{dW^*}) \cdot \frac{dW^*}{dW}$  as a default choice. While the result above is merely presented on the simple MNIST dataset, we observed similar behaviour on other experiments presented.

## B Inherent sparsity/One-shot pruning

We show hyperparameters for for MNIST and CIFAR-10 in Table 6. The MNIST values correspond to the motivating experiment in Section 3. For clarity, we include the one-shot experiment on ImageNet along with the more advanced sparsity techniques in Table 7. Our selection of hyperparameters was based on final performance of the dense model.

## C Advanced Pruning

Our implementation of TopKAST is based on code kindly provided to us by the authors, thus ensuring reproducibility of published results. While we were unable to obtain a reference implementation for Iter. Pruning, we do include a comparison of our implementation to results published in [11]. Our results match published results closely. We suggest the small gap may be closed by a more extensive sweep over update intervals and the number of training iterations upon which pruning starts or stops respectively. For our experiments on ImageNet the treatment of the first and final layer in the network varies between different experimental protocols. As we apply Powerprop. in conjunction with various techniques we follow the protocol outlined below:

- **Iter. Pruning, Powerprop. + Iter. Pruning, TopKAST, Powerprop. + TopKAST** We follow the protocol in [11] “*We modify our ResNet-50 training setup to leave the first convolutional layer fully dense, and only prune the final fully-connected layer to 80% sparsity. This heuristic is reasonable for ResNet-50, as the first layer makes up a small fraction of the total parameters in the model and the final layer makes up only .03% of the total FLOPs.*”
- **Powerprop. + TopKast + ERK** We follow the ERK sparsity distribution for 80% & 90% global sparsity shown in [13] (Figure 12), which prunes both the first and final layer.

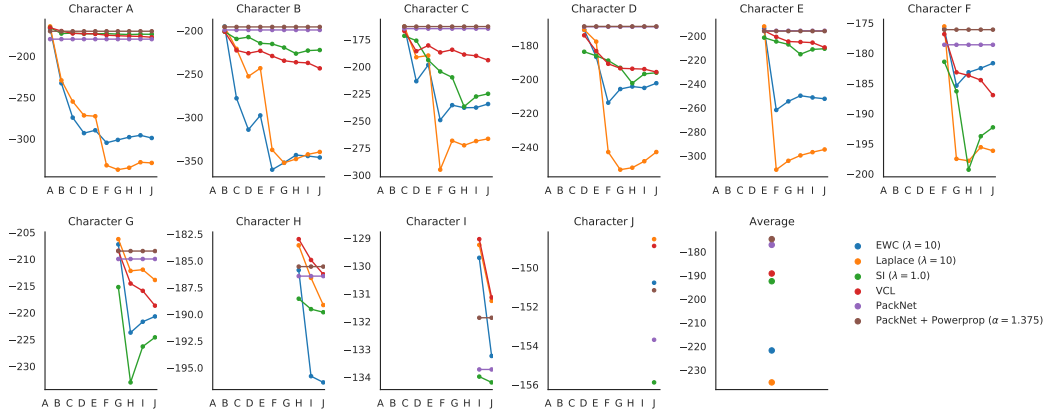


Figure 7: Test-LL results on notMNIST. The higher the better.

Furthermore, it is worth mentioning that it is customary to initialise the final (dense) layer to zero, which would make learning with Powerpropagation impossible due to the critical point property discussed in Section 2. Thus, we choose the initialiser in accordance with all other convolutional layers.

We show hyperparameters for our Imagenet experiments in Table 7. Note that we follow the learning rate schedule introduced by [90], where the learning rate is  $\eta = \eta_b 0.1 \cdot \frac{kn}{256}$  where  $\eta_b$  is the base learning rate (0.1 by default) and  $kn$  is the minibatch size.

## D Continual Learning on Deep Generative Models

Figures 6 & 7 show full results for the Continual Learning experiment with Deep Generative Models introduced by [46]. Note that catastrophic forgetting is eliminated by construction for approaches involving PackNet (due to the masking of gradients), explaining the improved performance. We also show a summary of the hyperparameters required to replicate the results in Table 8. We choose the best hyperparameters based on results on the validation set before computing final test-set results (using 5,000 MC samples to approximate the log-likelihood) using the best values previously chosen.

Our method was built on top of the published code (<https://github.com/nvcuong/variational-continual-learning>). The MNIST [41] dataset was downloaded from <http://yann.lecun.com/exdb/mnist/>, the notMNIST dataset is available here: <http://yaroslavvb.blogspot.com/2011/09/notmnist-dataset.html>.

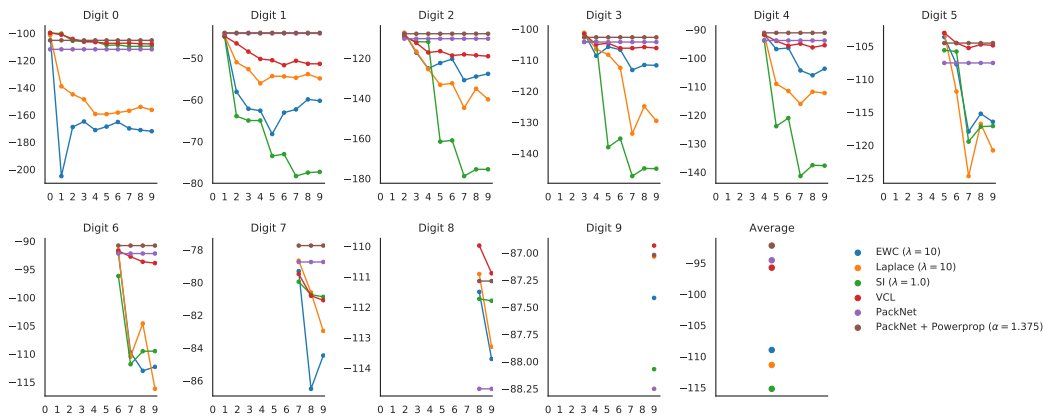


Figure 6: Test-LL results on MNIST. The higher the better.

## E Continual Reinforcement Learning

Our experiments on Reinforcement Learning follow the protocol in [79]. We built Powerprop. + Eff. PackNet on top of the authors’ code (<https://github.com/zajaczajac/cl-benchmark-tf2>). Note that due to computational constraints, we merely show results on six out of ten of the original CW10 task sequence. The full list of tasks is (in order of training):

- 1) 'hammer-v1'
- 2) 'push-wall-v1',
- 3) 'faucet-close-v1'
- 4) 'push-back-v1'
- 5) 'stick-pull-v1'
- 6) 'handle-press-side-v1'

A full description of each task is available in [91]. Hyperparameters are shown in Table 9 and were chosen based on the best results on the original three tasks, before running the final version on the full sequence. Note that we keep the vast majority of training settings unchanged. As the sparsity search procedure in Section 4 would include further interaction with the environment, we disable it for a fair comparison and reserve a fixed sparsity of 10% per task.

## F Task inference

Hyperparameters for the Class-Incremental learning versions of Permuted- and Split-MNIST are shown in Table 10 and for 10-task Split-Cifar100 in Table 11.

## G Hyperparameters

Table 6: Hyperparameters for the pruning experiments on MNIST & CIFAR-10.

Parameter	Considered range	Comment
<b>All Datasets</b>		
Activation function	$\{f(x) : \max(0, x) \text{ (ReLU)}\}$	[10]
Batch size	$\{60\}$	"
Pruning	$\{\text{Layerwise}\}$	"
Sparsity at output layer	$\{0.5 \times\}$	"
Initialisation	$\{\text{Gaussian Glorot}\}$	"
Optimiser	$\{\text{Momentum (0.9)}\}$	"
Learning rate	<b><math>\{0.0025\}</math></b>	"
Powerprop. $\alpha$	$\{2, 3, 4, 5\}$	Unstable for $\alpha > 5$
<b>MNIST specific</b>		
Network	$\{[784, 300, 100, 10]\}$	(LeNet) in [10]
Training steps	$\{50000\}$	"
<b>CIFAR-10 specific</b>		
Convolutions	$\{[64 \times 2, \text{pool}, 128 \times 2, \text{pool}, 256 \times 2, \text{pool}]\}$	(Conv-6) in [10]
Fully Connected Layer	$\{[256, 256, 10]\}$	"
Conv. Filters	$\{[3 \times 3]\}$	"
<i>pool</i>	$\{[\text{max-pooling (stride 2)}]\}$	"
Training steps	$\{100000\}$	"
Prune Batchnorm variables	$\{\text{False}\}$	"

Table 7: Hyperparameters for the experiments on ImageNet.

Parameter	Considered range	Comment
Network	ResNet-50	[4]
Batch size	{4096}	[14]
Training steps	{32000}	"
Learning rate ramp up epochs	{5}	"
Layerwise pruning?	{True}	"
Weight decay	{ $10^{-4}$ }	"
Label smoothing	{0.1}	"
Learning rate drops ( $\times 0.1$ ) after epochs	{[30, 70, 90]}	"
Initialise last year to zero? (All other methods)	{True}	
Initialise last year to zero? (TopKAST, Powerprop.)	{False}	
Optimiser	{Nesterov Momentum (0.9)}	
Batchnorm decay rate	{0.9}	
Prune Batchnorm variables	{False}	"
<b>Powerprop. + One-shot Pruning</b> specific		
Powerprop. $\alpha$	{1.125, 1.25, <b>1.375</b> , 1.5}	
Base Learning rate ( $\eta_b$ )	{0.1}	
<b>Powerprop. + Iter. Pruning</b> specific		
Base Learning rate ( $\eta_b$ )	{0.1, <b>0.4</b> , 0.5, 0.6}	
Start pruning after n% of training	{0, 10, <b>20</b> , 30}	
Stop pruning after n% of training	{70, <b>80</b> , 90, 100}	
Pruning interval	{2000}	
Powerprop. $\alpha$	{1.125, 1.25, <b>1.375</b> , 1.5, 2.0}	
<b>Powerprop. + TopKAST</b> specific		
Base Learning rate ( $\eta_b$ )	{ <b>0.1</b> , 0.4}	
Start pruning after n% of training	{0, 10, <b>20</b> , 30}	
Stop pruning after n% of training	{70, <b>80</b> , 90, 100}	
Pruning interval	{2000}	
Powerprop. $\alpha$	{1.125, 1.25, <b>1.375</b> , 1.5, 2.0}	

Table 8: Hyperparameters for the experiments on Deep Generative Models.

Parameter	Considered range	Comment
<b>Both Datasets</b>		
Network	{[784, 500, 500, 500, 100]}	[51]
Task specific decoder	{[50, 500, 500]}	"
Shared decoder	{[500, 500, 784]}	"
Activation function	{ $f(x) : \max(0, x)$ (ReLU)}	"
MC-Samples at Evaluation (All Methods)	{5000}	"
Batch size	{50}	"
dim( $z$ )	{50}	"
Regularisation strength ( $\lambda$ ) for EWC, Laplace	{1, 10, 100}	"
Regularisation strength ( $\lambda$ ) for SI	{1, 10, 100}	"
MC-Samples during Training (for VCL)	{10}	"
Freeze biases after first task?	{True}	"
$\gamma$ for EfficientPackNet?	{0.95}	"
Optimiser for VCL, SI, EWC, Laplace	Adam	"
Learning rate for Adam	{ $10^{-3}$ }	"
Optimiser (PackNet, All Powerprop. methods)	{Momentum (0.9)}	
<b>MNIST specific</b>		
Learning rate for Momentum	{[1, 2.5, 5, 7.5] $\cdot 10^{-3}$ , $10^{-2}$ }	
$\alpha$ for Powerprop.	{1.125, 1.25, 1.375, 1.5, 2.0}	See Table for best value.
Training epochs (SI)	{400}	"
Training epochs (all others)	{200}	"
<b>notMNIST specific</b>		
Learning rate for Momentum	{[1, 2.5, 5, 7.5] $\cdot 10^{-3}$ , $10^{-2}$ }	
$\alpha$ for Powerprop.	{1.125, 1.25, 1.375, 1.5, 2.0}	See Table for best value.
Training epochs (all)	{400}	"

Table 9: Hyperparameters for the experiments on Continual Reinforcement Learning.

Parameter	Considered range	Comment
Network	{[12, 256, 256, 256, 256]}	[79]
Actor output	{4}	"
Critic output	{1}	"
Activation	{Leaky ReLU}	"
Task-specific heads	{True}	" (Actor only)
Layernorm	{True}	"
Regularise critic	{False}	"
Reset Critic on Task Change	{True}	"
Batch size	{128}	"
Discount factor	{0.99}	"
Target output std. $\sigma_t$	{0.089}	"
Replay buffer size	{1M per task}	"
Replay buffer type	{FIFO}	"
Start training after	{1k steps}	" (for each task)
Train every	{50 steps}	"
Update steps	{50 steps}	" (i.e. 50 updates every 50 training steps)
Training steps	{1m/task}	"
Eff. PackNet re-train steps	{100k/task}	" (Using exiting replay data.)
Optimiser	{Adam}	"
Learning Rate	{ $10^{-3}$ }	"
Reset Optimiser on Task Change	{True}	"
Gradient norm clipping	{ $2 \cdot 10^{-5}$ , $10^{-3}$ }	
<b>Powerprop. + Eff. PackNet specific</b>		
Layerwise pruning?	{False, True}	
Sparsity range $S$	{[0.1]}	
Powerprop. $\alpha$	{1.125, 1.25, 1.375, 1.5}	
Re-initialise pruned weights?	{True}	

Table 10: Hyperparameters for the experiments on Permuted- &amp; Split-MNIST. EPN: Efficient PackNet

Parameter	Considered range	Comment
<b>All Datasets</b>		
Activation function	$\{f(x) : \max(0, x) \text{ (ReLU)}\}$	[51]
Task-specific heads?	{True}	"
Batch size	{64}	"
Pruning	{Layerwise, <b>Full Model</b> }	"
Optimiser	{SGD}	"
Sparsity range $S$	{[0.9, ... 0.3, 0.25 ... 0.15, 0.14, ... 0.01]}	"
] Convolutions	{[64 $\times$ 2, <i>pool</i> , 128 $\times$ 2, <i>pool</i> , 256 $\times$ 2, <i>pool</i> ]}	(Conv-6) in [10]
Fully Connected Layer	{[256, 256, 10]}	"
Conv. Filters	{[3 $\times$ 3]}	"
<i>pool</i>	{[max-pooling (stride 2)]}	"
Training steps	{100000}	"
Prune Batchnorm variables	{False}	"
Network	{[784, 1000, 1000, 10]}	[51]
Re-initialise pruned weights?	{True}	"
Target performance factor $\gamma$ for EPN	{0.9, 0.95, <b>0.99</b> , 0.995}	"
$\gamma$ for Powerprop. + EPN	{0.9, 0.95, <b>0.99</b> , 0.995}	"
Powerprop. $\alpha$	{1.125, 1.25, <b>1.375</b> , 1.5, 2.0}	"
Training steps per Task	{50000}	"
PackNet retrain steps	{0, <b>50000</b> }	"
Learning rate	{0.1, <b>0.05</b> , 0.01}	"
Network	{[784, 1000, 1000, 10]}	[51]
Re-initialise pruned weights?	{True}	"
Target performance factor $\gamma$ for EPN	{ <b>0.9</b> , 0.95, 0.99, 0.995}	"
$\gamma$ for Powerprop. + EPN	{ <b>0.9</b> , 0.95, 0.99, 0.995}	"
Powerprop. $\alpha$	{1.25, 1.375, <b>1.5</b> , 2.0}	$\alpha \geq 2.0$ unstable
Training steps per Task	{50000}	"
PackNet retrain steps	{50000}	"
Learning rate	{0.1, <b>0.05</b> , 0.01}	"

Table 11: Hyperparameters for the experiments on 10-task Split-Cifar100. EPN: Efficient PackNet

Parameter	Considered range	Comment
<b>All Datasets</b>		
Activation function	$\{f(x) : \max(0, x) \text{ (ReLU)}\}$	[84]
Task-specific heads?	{True}	"
Batch size	{64}	"
Pruning	{Layerwise, <b>Full Model</b> }	"
Optimiser	{SGD}	"
Sparsity range $S$	{[0.9, ... 0.3, 0.25 ... 0.15, 0.14, ... 0.01]}	"
] Convolutions	{[64, <i>pool</i> , 128, <i>pool</i> , 256, <i>pool</i> ]}	"
Fully Connected Layer	{[2048, 2048]}	"
Conv. Filters	{[4 $\times$ 4, 3 $\times$ 3, 2 $\times$ 2]}	"
<i>pool</i>	{[max-pooling (stride 2)]}	"
Batchnorm	{False}	"
Dropout	{0.2, 0.2, 0.5, 0.5, 0.5, 0.0}	Specifying rates per layer
Re-initialise pruned weights?	{True}	"
$\gamma$ for Powerprop. + EPN	{0.9, 0.95, <b>0.99</b> , 0.995}	"
Powerprop. $\alpha$	{1.375, 1.5, 1.625, <b>1.75</b> }	"
Training steps per task	{50000, <b>75000</b> }	"
PackNet retrain steps	{0, <b>Training steps</b> }	"
Learning rate	{0.1, <b>0.05</b> }	"